

# UC Santa Cruz

## UC Santa Cruz Previously Published Works

### Title

Seasonal Synechococcus and Thaumarchaeal population dynamics examined with high resolution with remote in situ instrumentation

### Permalink

<https://escholarship.org/uc/item/68s6q9h8>

### Journal

The ISME Journal: Multidisciplinary Journal of Microbial Ecology, 6(3)

### ISSN

1751-7362

### Authors

Robidart, Julie C  
Preston, Christina M  
Paerl, Ryan W  
et al.

### Publication Date

2012-03-01

### DOI

10.1038/ismej.2011.127

Peer reviewed

1 Seasonal dynamics of *Synechococcus* and *Thaumarchaeal* populations resolved with  
2 high resolution with remote *in situ* instrumentation

3

4 *Running title:* High resolution microbial oceanography

5

6 Julie C. Robidart<sup>1</sup>, Christina M. Preston<sup>2</sup>, Ryan W. Paerl<sup>1</sup>, Kendra A. Turk<sup>1</sup>, Annika C.  
7 Mosier<sup>3</sup>, Christopher A. Francis<sup>3</sup>, Christopher A. Scholin<sup>2</sup>, Jonathan P. Zehr<sup>1</sup>

8

9

10

11 <sup>1</sup>Department of Ocean Sciences, University of California Santa Cruz, 1156 High  
12 Street, Santa Cruz, CA 95064 USA

13 <sup>2</sup>Monterey Bay Aquarium Research Institute, 7700 Sandholdt Road, Moss Landing,  
14 CA 95039 USA

15 <sup>3</sup>Department of Environmental Earth System Science, 473 Via Ortega, Stanford  
16 University, Stanford, CA 94305-4216

17

18

19 **ABSTRACT**

20 Monterey Bay, California is an Eastern Boundary upwelling system that is nitrogen  
21 limited much of the year. In order to resolve population dynamics of  
22 microorganisms important for nutrient cycling in this region, we deployed the  
23 Environmental Sample Processor with quantitative PCR assays targeting both  
24 ribosomal RNA genes and functional genes for subclades of cyanobacteria  
25 (*Synechococcus*) and ammonia-oxidizing Archaea (*Thaumarchaeota*) populations.  
26 Results showed a strong correlation between *Thaumarchaea* abundances and  
27 nitrate during the spring upwelling but not the fall sampling period. In relatively  
28 stratified fall waters, the *Thaumarchaeota* community reached higher numbers than  
29 in the spring, and an unexpected positive correlation with chlorophyll concentration  
30 was observed. Further, we detected drops in *Synechococcus* abundance that  
31 occurred on short (i.e. daily) time scales. Upwelling intensity and blooms of  
32 eukaryotic phytoplankton strongly influenced *Synechococcus* distributions in the  
33 spring and fall, revealing what appear to be the environmental limitations of  
34 *Synechococcus* populations in this region. Each of these findings has implications for  
35 Monterey Bay biogeochemistry. High-resolution sampling provides a better-  
36 resolved framework within which to observe changes in the plankton community.  
37 We conclude that controls on these ecosystems change on smaller scales than are  
38 routinely assessed, and that more predictable trends will be uncovered if they are  
39 evaluated within seasonal (monthly), rather than on annual or interannual scales.

40 keywords: *Crenarchaeota*/Environmental Sample Processor/Monterey

41 Bay/*Synechococcus*/*Thaumarchaeota*/time series

42

## 43 INTRODUCTION

44 Ocean time series are essential for accurate predictions of climate scenarios  
45 in this age of anthropogenic change (Doney 1999). Marine biological time series  
46 have proven invaluable for uncovering major oceanographic trends that would not  
47 have been observed otherwise (Chavez 1999, Chavez *et al.*, 2003, Karl *et al.*, 1995,  
48 Karl 1999, Karl 2007, McGowan *et al.*, 1998). Although monthly time series are  
49 essential for providing data on annual and decadal patterns, the factors controlling  
50 changes in microbial populations are known to occur on shorter time, and smaller  
51 space scales (i.e. seconds to months, depending on the process: Karl and Dore 2001;  
52 Johnson *et al.*, 2009). However, sustaining high frequency assessments of microbial  
53 populations is generally not possible given logistical and practical constraints,  
54 particularly for remote locations. With few exceptions, acquisition of detailed  
55 information concerning microbial distributions and activities is typically limited to  
56 ship-based surveys. The reliance on traditional ship-based sampling has driven the  
57 development and testing of new biological sensors (Paul *et al.*, 2007, Scholin 2010,  
58 Shade *et al.*, 2009).

59 The Environmental Sample Processor (ESP) is among this new generation of  
60 sensors. Modeled as an 'ecogenomic sensor' (Scholin 2010), the instrument  
61 provides for subsurface, hands-off collection of discrete water samples, particle  
62 concentration and application of various molecular biological analyses, including  
63 quantitative PCR (Preston *et al.*, 2011) as well as DNA and protein probe arrays for  
64 detection of a variety of organisms, genes and metabolites (Goffredi *et al.*, 2006;  
65 Greenfield *et al.* 2008; Haywood *et al.*, 2007; Doucette *et al.*, 2009; Preston *et al.*,

66 2009; Scholin *et al.*, 2009; Scholin 2010). At present, the instrument can perform  
67 these types of assays with daily resolution and in real-time, and transmit data to a  
68 remote location. The ESP can also archive samples for more in-depth analyses upon  
69 instrument retrieval (Ottesen *et al.*, 2011; Scholin *et al.*, 2009).

70 Monterey Bay, California serves as an optimal location for a high resolution  
71 time series study, as it has been historically monitored by the Monterey Bay  
72 Aquarium Research Institute (MBARI) time series (Pennington and Chavez 2000),  
73 and is a region of enormous biogeochemical interest with strong seasonality in  
74 environmental conditions (Breaker and Broenkow 1994). Productivity in Monterey  
75 Bay is nitrogen-limited for much of the year (Johnson *et al.*, 2006). Upwelling is the  
76 primary source of nitrate, and remineralization within the surface waters adds to  
77 the nitrogen pool during productive and stratified periods (Dugdale and Goering  
78 1967; Johnson *et al.*, 2006). Eukaryotic and some cyanobacterial phytoplankton can  
79 assimilate nitrate as well as ammonia, and compete with each other for limiting  
80 nitrogen in the bay.

81 The *Thaumarchaeota* (or Group I Archaea, formerly the *Crenarchaeota*  
82 (Brochier-Armanet *et al.*, 2008; Spang *et al.*, 2010)) also play an important role in  
83 the nitrogen cycle in coastal marine systems by oxidizing ammonia to nitrite  
84 (Konneke *et al.*, 2005) , thus altering the form of nitrogen available for  
85 photosynthesis and other processes in upwelled waters and deeper in the photic  
86 zone (where they reside: Mincer *et al.*, 2007; Santoro *et al.*, 2010; Preston *et al.*,  
87 2011) . The *Thaumarchaeota* have widespread global distributions, and have been  
88 estimated to comprise over 20% of marine picoplankton (Karner *et al.*, 2001).

89 These organisms are key nitrifiers in Monterey Bay (Francis *et al.*, 2005; Mincer *et*  
90 *al.*, 2007; Santoro *et al.*, 2010) and maintain large, but temporally variable  
91 populations in coastal California waters (Massana *et al.*, 1997; Mincer *et al.*, 2007;  
92 Murray *et al.*, 1999).

93 The cyanobacteria are significant contributors to marine primary production  
94 (Goericke and Welschmeyer 1993; Liu *et al.*, 1997) and perform many essential  
95 functions to maintain the health of food webs (Wilhelm and Trick 1994; Zehr *et al.*,  
96 2001). The cyanobacterial genus *Synechococcus* can assimilate a diversity of  
97 nitrogen compounds, including ammonium and nitrate, and reside in relatively  
98 nutrient-rich waters at coastal sites throughout the world (Scanlan and West 2002).  
99 The *Synechococcus* populations in coastal California waters are genetically diverse  
100 (Paerl *et al.*, 2008; Palenik *et al.*, 2009; Toledo and Palenik 1997) and strain  
101 abundances vary over the course of the year (Paerl *et al.*, in review; Tai and Palenik  
102 2009).

103 Despite their important roles in marine nutrient cycling, *Thaumarchaeota*  
104 and *Synechococcus* population dynamics in Monterey Bay are not well resolved. In  
105 an effort to better understand controls on these organisms' distributions, we  
106 deployed an ESP in the spring and fall months of 2009 in shallow waters at the  
107 MBARI's coastal time series station M0. This study applies qPCR assays to detect  
108 both general groups of organisms as well as specific subclades to determine trends  
109 in microbial distribution relative to environmental change. Physical, chemical and  
110 biological parameters were measured over 57 days, along with the corresponding  
111 changes in the prokaryotic communities using the ESP. *Thaumarchaeota* were

112 detected with a general 16S rRNA assay (Suzuki *et al.*, 2000) and subclades were  
113 enumerated with a functional gene assay targeting the ammonia monooxygenase  $\alpha$ -  
114 subunit gene for the marine shallow water ecotype (*amoA*, group A; Mosier and  
115 Francis 2011). *Synechococcus* were detected with a comprehensive *rbcL* assay  
116 targeting the ribulose-1,5-bisphosphate carboxylase gene that accounts for ca. 89%  
117 total *Synechococcus* in Monterey Bay when compared with flow cytometry derived  
118 cell counts (Paerl *et al.*, in review) (Preston *et al.*, 2011), while *Synechococcus*  
119 subclades were detected with a functional gene assay coding for the assimilatory  
120 nitrate reductase gene (*narB*) and targeting subclades C C1 and D C2 (associated  
121 with *Synechococcus* clades I and IV, respectively from cultured isolates: Paerl *et al.*,  
122 2011).

123         The utility of the ESP for quantifying microbial population dynamics in  
124 Monterey Bay has been demonstrated by Preston *et al.*, 2011, where microbes with  
125 predictable dynamics were quantified during the upwelling season, for technical  
126 validation of the ESP technology. Here it was shown that *Thaumarchaeota*  
127 abundances increase with upwelling, as expected based on their deeper  
128 distributions. Aside from this proof-of-concept field study, their abundance near  
129 shore has not been addressed, and it is generally assumed based on previous  
130 findings offshore (Santoro *et al.*, 2010; Mincer *et al.*, 2007) that the *Thaumarchaea*  
131 are scarce, if at all present in shallow waters, and that any distribution to shallow  
132 waters is determined by upwelling and mixing alone. Paerl *et al.*, have shown that  
133 *Synechococcus* populations are abundant for most of the year near the coast, with  
134 population decreases corresponding with times of intense upwelling (Paerl *et al.*, in

135 review), and a fairly consistent presence in surface water otherwise. With daily  
136 sampling, Preston et al. 2011 further resolved the period of *Synechococcus*  
137 appearance in coastal waters, at the relaxation of upwelling. Little is known,  
138 however, regarding the drivers of specific *Synechococcus* subclade distributions over  
139 the rest of the year, nor whether their populations are consistently present when  
140 upwelling intensity is low. This study sought to obtain higher resolution of the  
141 abundance of both *Thaumarchaeal* and *Synechococcus* populations and subclades,  
142 within and between seasons. The resulting data illustrate a highly dynamic  
143 microbial community reflective of regional scale physical processes, such as  
144 upwelling, as well as localized processes in stable conditions, where we posit that  
145 inter-organismal interactions play a determinant role in dictating microbial  
146 distributions.

147

148

## 149 **METHODS**

150 Instruments were deployed in Monterey Bay, CA at Station M0 (36.83N,  
151 121.90W) on a mooring as described previously (Doucette *et al.*, 2009). ESP  
152 deployments occurred in the spring (May 14 to June 11) and fall (September 24 to  
153 October 28) of 2009, and included an attached CTD (Seabird SBE 16+CTD, Bellevue,  
154 WA) with fluorometer (Turner Cyclops-7) and transmissometer (WetLABS Cstar).  
155 An *in situ* ultraviolet spectrophotometer (ISUS; (Johnson and Coletti 2002) was also  
156 coupled to the ESP for *in situ* nitrate analyses. Data was recorded every 12 minutes  
157 from accompanying sensors. Data was transmitted to shore in real time over a radio



158 modem. The instrument was deployed slightly deeper in the spring (10-11.4 m)  
159 than the fall (5.8-8.8 m).

160 *Instrument preparation*

161 To prepare the ESP, tubing was cleaned and reagents were loaded as  
162 described (Preston *et al.*, 2011). Quantitative PCR assays were loaded onto the  
163 microfluidic block for the following genes: *Thaumarchaeota* 16S rRNA (which  
164 amplifies all ammonia oxidizing Archaea known; Preston *et al.*, 2011), and *amoA*  
165 water column group A (which target all known *amoA* group A sequences from a  
166 Monterey Bay database, representing 825 sequences from a total of 9634): Mosier  
167 and Francis 2011), *Synechococcus* RuBisCO (*rbcL*, targets all cultivated  
168 *Synechococcus* clades I-IV and all known *rbcL* sequences in Monterey Bay (Paerl *et*  
169 *al.*, in review)), *narB* group C\_C1 and group D\_C2 ((Paerl *et al.*, 2011). The *narB* and  
170 *rbcL* assays were the same: each 30µl reaction contained 1x Accuprime Supermix II  
171 (Invitrogen, Carlsbad, CA), 0.333 µM primers, and 2µM probe. The *amoA* group A  
172 assay contained 1x Accuprime, 2.5 mM additional MgCl<sub>2</sub>, 0.5 µM forward primer,  
173 and 0.333 µM reverse primer. 16S rRNA amplification and cycling conditions were  
174 as described previously (Preston *et al.*, 2011). For enumeration, the deployed  
175 reagents were used on the microfluidic block of the ESP to create duplicate standard  
176 curves from 10-fold linearized plasmid standard dilutions ranging from 10<sup>2</sup>-10<sup>5</sup> or  
177 10<sup>6</sup> gene copies per reaction. Amplification plots were analyzed and standard  
178 curves generated in Excel. Quantitative PCR assay cross-reactivities were low or  
179 nonexistent (published in Paerl *et al.*, in review; Preston *et al.*, 2011) and Mosier and  
180 Francis 2011) and detection limits on the microfluidic block were ca. 10-20

181 copies/ml for *Synechococcus* targets, 10-50 copies/ml for *Thaumarchaeal* targets.  
182 qPCR standard curve information for the spring deployment are reported elsewhere  
183 (Preston *et al.*, 2011). For the fall deployment, copy numbers for the standards in  
184 each assay were linear with cycle threshold ( $C_t$ ). Linear regressions for all assays  
185 had  $r^2$  values of  $>.98$ , and amplification efficiencies were 90-110% with the  
186 exception of the *narB* group C C1 assay, which had an efficiency of 88.6%. Analyses  
187 of this target group are discussed with consideration of the implications of this  
188 lower reaction efficiency. The DNA extraction efficiency in the ESP microfluidic  
189 block was 98-104% compared to parallel extractions performed in the lab with a  
190 Qiagen DNeasy Kit.

191 ESP operations included 24 discrete sampling events in which particles  
192 retained on 0.22  $\mu\text{m}$  pore size filters were subjected to qPCR analyses, and an equal  
193 number of discrete sampling events where particulates were preserved for later  
194 analysis (after Ottesen *et al.*, 2011). The day before each deployment (on May 14  
195 and September 23), 50 ml of sterile water (Sigma-Aldrich) was sampled by the  
196 intake of the instrument in order to determine the degree of internal contamination,  
197 if any. Negative controls were also run during each deployment (on May 17 and 30  
198 in the spring and October 9 and 16 in the fall), each containing a core system  
199 negative control (where a “negative lysate” is created and run through the entire  
200 system) and a no-template control (NTC: where the PCR is run with the elution  
201 water used for DNA extractions in normal operating conditions).

202 *Assay performance during deployment*

203            Though the ESP does not allow standard curve generation for all samples  
204 taken for all assays while deployed, internal positive controls give some degree of  
205 confidence in target quantification on a per sample basis. For each sample, the  
206 degree of PCR inhibition was assessed using a positive control reaction as described  
207 in Preston *et al.*, 2011. Samples were only included in our analyses if the  $C_t$  of the  
208 internal positive control (IPC) was between 33.5 and 36.5 (spring) or 27.2 and 29.7  
209 (fall). These ranges were within the  $C_t$  variability encountered for each PCR module  
210 in reactions with water; the template of the IPC is included in the primer/probe  
211 reagent. None of the NTC reactions amplified indicating uncontaminated reagents  
212 and sufficient cleaning of the PCR microfluidics between samples.

213            In core system negative control reactions, amplification occurred for a few of  
214 the targets. However, in each case, the  $C_t$  values translated to copy numbers that  
215 were at least an order of magnitude lower than the sample, which does not affect  
216 our interpretations of the trends. The fall deployment allowed interrogation of  
217 subpopulations of both *Synechococcus* and *Thaumarchaeota*. Subclade dynamics  
218 correlated with total clade dynamics, providing support that these groups were  
219 adequately quantified. Pearson and Spearman correlation analyses were performed  
220 using SigmaPlot 11.2 (Systat Software, Inc.).

#### 221 *Additional data*

222            Mooring data from station M1 (Pennington and Chavez 2000) was used to  
223 create the water column profiles for Monterey Bay, and chlorophyll satellite images  
224 were obtained from Moderate Resolution Imaging Spectroradiometer (MODIS) on  
225 NOAA's Coastwatch/SWFSC Oceanwatch Live Access Server

226 (<http://coastwatch.pfeg.noaa.gov>).

227

## 228 **RESULTS/DISCUSSION**

### 229 **Seasonal conditions at station M0**

230       Seasonal upwelling dominated spring conditions at Station M0, leading to  
231 two major bloom periods that were clearly distinguished by increased chlorophyll-*a*  
232 fluorescence (Figure 1). During this deployment period, conditions developed from  
233 initial intense upwelling to relaxation and eventual stratification of the water  
234 column (Figures 1, 2). The first week of the deployment, when upwelling was  
235 sustained, high nitrate concentrations (near 25 $\mu$ M), high salinity (ca. 33.9 PSU) and  
236 low temperatures (<11°C) were observed as expected (Breaker and Broenkow  
237 1994); (Figures 1, 2). As a reflection of deep-water transport to surface waters  
238 (Bolin and Abbott 1963), chlorophyll-*a* concentrations were low and constant  
239 (below 10  $\mu$ g/L) until the relaxation of upwelling around May 24. The following  
240 seven ESP-collected biological samples after this date were from periods of high  
241 chlorophyll-*a*/low transmissivity (until ca. June 2: black-outlined boxes Figure 3),  
242 indicating abundant eukaryotic phytoplankton at station M0 (Behrenfeld and Boss  
243 2006; Green and Sosik 2004; Green *et al.*, 2003). These blooms were not adequately  
244 captured by satellite imaging (<http://coastwatch.pfeg.noaa.gov>; Figure 1), but  
245 microscopy of Monterey Bay seawater during this period supports this  
246 interpretation with the identification of a bloom of *Chaetoceros* spp. on May 27  
247 [HABMAP: <http://cimt2007plankton.wordpress.com/>]. A tongue of nitrate-rich,  
248 low salinity, offshore water entered the bay displacing the bloom (Preston *et al.*,

249 2011), and this was followed by increased stratification that persisted through the  
250 end of the deployment when nitrate dropped to 5-10  $\mu\text{M}$ , salinity to 33.6 PSU, and  
251 temperatures raised to 13-14°C (Figure 1). There was only trace precipitation over  
252 the course of the spring deployment.

253         After an initial unstable phase that lasted 3 days, fall conditions were well-  
254 stratified relative to spring, with warmer (12-15°C), fresher (33.2-33.5 PSU) water,  
255 steady physical and chemical conditions and no deep-water supply to the surface  
256 detected (Figures 1, 2). Nitrate was less variable in the fall than the spring, with  
257 concentrations ranging from 8-12  $\mu\text{M}$  with the exception of several transient  
258 (hourly) spikes to ca. 17 $\mu\text{M}$ . Chlorophyll-*a* concentrations increased over time,  
259 beginning at an average of 7  $\mu\text{g/L}$  (with a range from approximately 3-20  $\mu\text{g/L}$ ), and  
260 increasing to an average of 17  $\mu\text{g/L}$  (9-38  $\mu\text{g/L}$  range; Figure 1, 2). The ratio of  
261 chlorophyll-*a* to % transmission during ESP sampling periods was high, indicating  
262 abundant eukaryotic phytoplankton for most of the fall (Figure 3; (Behrenfeld and  
263 Boss 2006, Green and Sosik 2004); (Green *et al.*, 2003). Microscopy of Monterey Bay  
264 seawater for this period also documented high abundances of eukaryotic  
265 phytoplankton, with dinoflagellates (*Ceratium* spp.) dominating for the majority of  
266 the deployment period (sampled at Santa Cruz Wharf on Sep 23, 29; Oct 5, 12, 19:  
267 <http://cimt2007plankton.wordpress.com/>), and *Pseudonitzschia*-like diatoms  
268 observed in high numbers for one of the five samples (on October 5  
269 <http://cimt2007plankton.wordpress.com/>). There was only trace precipitation over  
270 this period, with the exception of 4.54 inches of rain on October 13. This rain event

271 was coincident with the onshore influx of a chlorophyll-poor water mass (Figure 3,  
272 outlined diamonds).

273

#### 274 **Microbial population dynamics**

275 Upwelling was the major driver of microbial distributions in the spring, as  
276 expected, but population abundances fluctuated despite the relative stability of the  
277 water column in stratified fall conditions. Our data lead us to hypothesize that  
278 blooms of eukaryotic phytoplankton have an effect on the *Thaumarchaeota* and  
279 *Synechococcus* clade dynamics over this period.

#### 280 **Thaumarchaeal population dynamics**

281 For much of the spring period, the *Thaumarchaeota* were abundant in  
282 surface waters, based on 16S rRNA gene copy numbers (with a range of  
283 undetectable to ca.  $6.0 \times 10^4$  copies per ml; (Preston *et al.*, 2011). A weak negative  
284 correlation with chlorophyll-*a* during this upwelling period likely reflects the  
285 transport of chlorophyll-poor, *Thaumarchaea*-rich deep-water to the surface  
286 (Pearson's  $r = -0.448$ ,  $P = 0.037$ ; Spearman's correlation insignificant).

287 *Thaumarchaeota* abundances were positively correlated with the magnitude of  
288 upwelling, using temperature (Pearson's  $r = -0.636$ ,  $P = 0.001$ ; Spearman's  $\rho = -0.853$ ,  
289  $P < 0.0001$ ), salinity (Pearson's  $r = 0.558$ ,  $P = 0.007$ ; Spearman's  $\rho = 0.704$ ,  $P = 0.0002$ )  
290 and nitrate as a proxy (Figure 4A; Pearson's  $r = 0.769$ ,  $P < 0.0001$ ; Spearman's  
291  $\rho = 0.831$ ,  $P < 0.0001$ ). Aside from one exception, all quantified genes show  
292 correlations with these three upwelling proxies in the spring, demonstrating the  
293 impact of upwelling on these microbial populations. *Synechococcus*, however, did

294 not correlate with nitrate (see below), and the observation that *Thaumarchaeal*  
295 abundances correlate most strongly with nitrate (vs. temperature and salinity) may  
296 reflect their role in marine nitrification.

297 *Thaumarchaeota* were more abundant in the fall (16S rRNA gene range of ca.  
298  $2.7 \times 10^3$  to  $1.3 \times 10^6$  per ml), and again correlated with cold (Pearson's  $r = -0.754$ ,  
299  $P = 0.0002$ ; Spearman's  $\rho = -0.805$ ,  $P < 0.0001$ ), saline waters (Pearson's  $r = 0.625$ ,  
300  $P = 0.004$ ; Spearman's  $\rho = 0.853$ ,  $P < 0.0001$ ), but the connection between  
301 *Thaumarchaeal* abundance and nitrate concentration was not supported in these  
302 stratified conditions. Also in contrast to the spring, *Thaumarchaea* 16S rRNA genes  
303 showed a significant positive correlation with chlorophyll-*a* in the fall (Pearson's  
304  $r = 0.554$ ,  $P = 0.014$ ; Spearman's  $\rho = 0.721$ ,  $P = 0.0003$ ) (Figure 4A). During this time,  
305 large *Thaumarchaeal* populations were sustained in the surface waters and 16S  
306 rRNA gene copy numbers grew to become two orders of magnitude more abundant  
307 over time (Figure 4A). These data suggest that *Thaumarchaeal* populations can  
308 thrive in surface waters during blooms of eukaryotic phytoplankton. The decrease  
309 in abundance that correlates with a drop in chlorophyll towards the end of the  
310 deployment may be a reflection of the chlorophyll-poor water mass that moved  
311 onshore at this time (which was warmer and less saline, two conditions previously  
312 suggested to be unfavorable based on marine *Thaumarchaea* distributions ((Mincer  
313 *et al.*, 2007, Murray *et al.*, 1999, Santoro *et al.*, 2010)).

314 In order to determine whether the *Thaumarchaea* targeted by the 16S rRNA  
315 gene primers used in this study have the genetic potential to oxidize ammonia, we  
316 correlated their abundance with the abundance of ammonia monooxygenase

317 subunit A functional genes (*amoA*). There is now considerable evidence for the  
318 existence of two distinct clades of marine ammonia oxidizing Archaea (AOA),  
319 namely the ‘shallow’ (group A) and ‘deep’ (group B) water column AOA (Francis *et al.*,  
320 2005; Hallam *et al.*, 2006; Beman *et al.*, 2008; Mosier and Francis 2011). It is worth  
321 noting that both marine water column *amoA* subclades would be detected by the  
322 described *Thaumarchaeal* 16S rRNA qPCR assay. In this study, we specifically  
323 targeted the shallow (group A) water column AOA ecotype, and during stratification  
324 in the fall season. Previous work in the Monterey Bay region shows relative  
325 consistency between total *amoA* gene and marine Group I 16S rRNA gene  
326 abundances (Santoro *et al.*, 2010), implying that most, if not all, of the  
327 *Thaumarchaea* contain at least one copy of the *amoA* gene.

328         Though *Thaumarchaeota* subclade populations have not been quantified at  
329 depths relevant to this study (5-10 m), or near shore within Monterey Bay, trends  
330 from past studies in the region (Mincer *et al.*, 2007, Santoro *et al.*, 2010) would  
331 imply that the shallow water subclade A might dominate in surface waters at station  
332 M0. We find that this subclade is abundant for the duration of the fall deployment  
333 (ca.  $2.1 \times 10^3$  to  $7.5 \times 10^4$  copies per ml), but the ratio of *amoA*, group A to 16S rRNA  
334 gene copy numbers ranges from 0.05 to 1.39, with an average of 0.26 (these  
335 numbers are not directly comparable to ratios found in past studies, since those  
336 enumerated total *amoA* group A and B abundances rather than that of group A only  
337 (Mincer *et al.*, 2007; Santoro *et al.*, 2010)). For just six time points, the shallow  
338 subclade A makes up >50% of the *Thaumarchaea* 16S rRNA copy number. This  
339 corresponds with the lowest chlorophyll-*a* concentrations (Figure 4B) after



340 movement of the offshore water mass into the bay, leading to the hypothesis that  
341 the shallow subclade is dominant in shallow waters offshore, but that we are  
342 missing the *amoA* diversity (e.g., 'deep' subclade or otherwise), closer to the coast.  
343 Future deployments will measure *amoA* diversity at this site and target all subclades  
344 in stratified fall conditions, in order to determine the relative contribution of each to  
345 the total *Thaumarchaeal* community.

346         In a previous California coastal time series study, *Thaumarchaeal*  
347 abundances correlated with the characteristics of deeper waters, including low  
348 temperature, high salinity and low chlorophyll (Murray *et al.*, 1999). Murray *et al.*,  
349 present correlative data from 32 months integrated over the course of the time  
350 series, so any potential short-term effects may have been overlooked. Furthermore,  
351 though longer in duration than this study, the previous study has monthly temporal  
352 resolution, while this study has daily resolution. Despite these differences, we  
353 expected the trends to be similar: large *Thaumarchaeal* abundances in the spring  
354 that correlate with upwelling, and low numbers in the fall as a result of increased  
355 water column stratification. While the expected trends were indeed observed in the  
356 spring, the higher relative abundance of the *Thaumarchaea* populations in the fall  
357 points to additional unforeseen factors dictating their distributions. Repeated  
358 observation of this phenomenon as a result of higher resolution sampling, affords  
359 sufficient confidence to investigate the cause behind this finding in the near future.

360         The high abundance of *Thaumarchaea* in the surface waters at this coastal  
361 station during stratification has far reaching implications. If this correlation  
362 between the *Thaumarchaea* population and chlorophyll-*a* holds true during

363 nutrient-rich stratified conditions in Monterey Bay, then we would expect near  
364 shore regions to experience several periods of *Thaumarchaeal* dominance annually,  
365 perhaps up to 3-4 months per year (Breaker and Broenkow 1994). Assuming that  
366 this population is oxidizing ammonia, it is competing with phytoplankton for this  
367 preferred nitrogen source where nitrogen is limiting. Furthermore, the relative  
368 decrease in ammonia and increase in nitrite (and therefore nitrate) might sustain  
369 growth of larger phytoplankton in the bay (L'Helguen *et al.*, 2008) and thereby  
370 contribute to increased carbon export during these periods (Yool *et al.*, 2007).

### 371 ***Synechococcus* population dynamics**

372 Over the two months (spring and fall) of ESP sampling at station M0, *rbcL*-  
373 based *Synechococcus* abundance estimates ranged from undetectable to  $10^4$  genes  
374 per ml. The only correlations in the spring included a positive relationship between  
375 *Synechococcus* abundance and temperature (Pearson's  $r=0.708$ ,  $P=0.0002$ ;  
376 Spearman's  $\rho=0.708$ ,  $P=0.0002$ ), as well as a negative relationship with salinity  
377 (Pearson's  $r=-0.567$ ,  $P=0.006$ ; Spearman's  $\rho=-0.758$ ,  $P<0.0001$ ), likely reflecting the  
378 inability of *Synechococcus* to remain in surface waters during active upwelling. Once  
379 upwelling ceased and conditions became more uniform, *Synechococcus* increased to  
380  $2.4 \times 10^3$  copies per ml over the course of three days (Figures 1, 2).

381 We observed no correlation between *Synechococcus* abundances and any of  
382 the environmental parameters measured over the fall period. Though the water  
383 column was stratified throughout the fall and there was very little change in the  
384 physico-chemical environment, major drops in *Synechococcus* abundance (from  $10^4$   
385 to  $<10$  per milliliter over one day) were observed twice during this time. These

386 crashes coincided with spikes in chlorophyll (Figure 5, time points with thick black  
387 dotted outlines), and may be the result of competition or grazing. In a southern  
388 California coastal time series, total *Synechococcus* abundances correlated weakly  
389 with temperature, and a weaker negative correlation was observed with phosphate  
390 concentration (Tai and Palenik 2009). It is likely that different parameters control  
391 *Synechococcus* distribution over the course of the year in Monterey Bay. In the  
392 future we hope to deploy more physical and chemical sensors, including phosphate  
393 and ammonia sensors, in order to further resolve the environmental context during  
394 these time series.

395       Only a narrow range of chlorophyll-*a* and nitrate concentrations were  
396 sampled during the spring and fall ESP series, representing 18.5% of the range  
397 sampled by MBARI's Biological Oceanography Group at station M0 over the course  
398 of four years (2006-2010; Figure 5). We found that *Synechococcus* abundances were  
399 highest over a predictable range, specifically less than ca. 16 $\mu$ M nitrate and 15 $\mu$ g/L  
400 chlorophyll-*a*. The only exceptions to this included the period of upwelling  
401 relaxation in the spring when conditions were still erratic and *Synechococcus* was  
402 not yet abundant (demarcated in Figure 1A, and corresponding to the few small  
403 dashed circles within the box in Figure 5), and a single time point in the fall where  
404 chlorophyll concentrations were highest (26.6  $\mu$ g/L). It appears that the  
405 environmental parameters recorded during our deployments were more extreme  
406 than typical conditions at this coastal station, and we may have sampled the upper  
407 limits of *Synechococcus* distribution with respect to nitrate and chlorophyll-*a*  
408 concentration at Station M0. We intend to continue deploying over various times of

409 year in order to sample a higher diversity of conditions, to gather data on  
410 *Synechococcus* distributions under more common circumstances and to test whether  
411 the observed trends hold true.

412 Previous time series in Monterey Bay demonstrate the degree of variation  
413 observed for *Synechococcus* populations over the year, with total abundances  
414 ranging from undetectable to  $10^5$  copies per ml seawater, and peak abundances  
415 occurring over the summer and throughout the fall and winter (Paerl *et al.*, in  
416 review). Daily sampling with the Environmental Sample Processor further resolves  
417 *Synechococcus* population dynamics, and it is apparent that the population does not  
418 maintain continuously high abundances over the summer and fall periods in  
419 Monterey Bay.

420 *Synechococcus* clades I and IV appear to be common in temperate coastal  
421 waters (Paerl *et al.*, in press, Zwirgmaier *et al.*, 2008). In the fall of our time series,  
422 *narB* was used to differentiate between the dominant *Synechococcus* groups C\_C1  
423 (part of clade I) and D\_C2 (of clade IV). Previously in Monterey Bay, these groups  
424 maintained relatively high abundances, with subgroup D\_C2 being slightly more  
425 abundant during 2006 and 2008 (Paerl *et al.*, in review). These *narB* subgroups  
426 were also found to be most abundant in the coastal-transition and upwelling zones  
427 of the California Current System (CCS), and low in abundance in oligotrophic waters  
428 further offshore (Paerl *et al.*, 2011).

429 Unlike average conditions in the previous study, here we find that group  
430 C\_C1 (clade I) is slightly numerically dominant over clade D\_C2. Representative  
431 *Synechococcus* strains from clade I and IV differ in their gene repertoires (Dufresne

432 *et al.*, 2008) so there is the genetic potential for the presence of these different  
433 subgroups to have implications for ecosystem function or nitrogen cycling in this  
434 region. Both groups are lower in abundance in offshore waters (Figure 6A, and low  
435 salinity waters in Figure 6B). This contradicts what might be expected based on  
436 previously described higher distributions of *Synechococcus* in offshore waters  
437 (Paerl *et al.*, in press), though a likely explanation is that these sampled waters were  
438 not from CCS transition waters. The relative population sizes of each subclade  
439 demonstrate no clear differences with respect to temperature or salinity  
440 preferences for either subclade (Figure 6B). Though these were the only subclades  
441 quantified, the *rbcL* copy number remains high when *narB* groups C\_C1 and D\_C2  
442 numbers decrease, indicating the presence of additional subclade(s) in offshore  
443 waters.

#### 444 **Conclusions**

445 Owing to high-resolution sampling, we have demonstrated that high  
446 *Thaumarchaea* abundances can be seen in the stratified fall surface waters, and that  
447 these abundances can exceed *Thaumarchaea* numbers transported to surface  
448 waters during active upwelling. Such high abundances of ammonia oxidizers likely  
449 have significant implications for local nitrogen cycling. If the mass of data we  
450 retrieved from the *Thaumarchaeota* in the fall series were instead a single data  
451 point in one month, over the course of a year time series, we may have disregarded  
452 it as an outlier, since the conditions corresponding with these high abundances are  
453 not conditions that normally coincide with abundant *Thaumarchaeota*. These data  
454 demonstrate that *Thaumarchaeota* reside with abundant phytoplankton in the

455 surface waters over long periods of time, however it is currently unknown whether  
456 this co-occurrence is typical in stratified waters in Monterey Bay. It is now possible  
457 to test this theory by sampling high and low chlorophyll regimes within the same  
458 water mass during stratified conditions, using adaptive sampling with robotic  
459 instrumentation.

460         The daily resolution of the Environmental Sample Processor also allowed us  
461 to demonstrate higher variability in *Synechococcus* populations in the fall than  
462 anticipated based on previous time series with approximately monthly resolution.  
463 Due again to the high number of samples within this season, we were successful in  
464 linking low *Synechococcus* numbers to high chlorophyll concentration, indicating a  
465 possible inverse relationship between bloom conditions and *Synechococcus*  
466 abundances. Here, we have demonstrated the deeper insight gained through high-  
467 resolution biological sensing, without the need for continuous on-station ship-time.

468         The sampling frequencies of most time series programs necessitate a more  
469 general interpretation of microbial dynamics and though seasonal trends may be  
470 investigated, factors that are important for biogeochemistry are easily obscured by  
471 the low likelihood of their continued observation due to intermittent sampling. We  
472 have shown that the factors driving *Synechococcus* and *Thaumarchaea* population  
473 dynamics changed between seasons, and such effects that occur over shorter scales  
474 can be easily overlooked when only investigating the dominant drivers on annual or  
475 interannual cycles.

476

477 **ACKNOWLEDGEMENTS**

478 This work was partially funded by the MEGAMER facility grant by the Gordon and  
479 Betty Moore Foundation and the NSF Center for Microbial Oceanography, Research  
480 and Education (C-MORE) (to J.P.Z.). Development and application of the ESP has  
481 been funded in part by grants (to C.A.S.) from the David and Lucille Packard  
482 Foundation (through funds allocated to MBARI), NSF, NASA Astrobiology, and the  
483 Gordon and Betty Moore Foundation. Work was also supported in part by an EPA  
484 STAR Graduate Fellowship and Stanford University DARE Fellowship (to A.C.M.), as  
485 well a National Science Foundation grant (OCE-0825363) to C.A.F. We thank the  
486 science and engineering technicians and machinists at MBARI (in particular Cheri  
487 Everlove and Roman Marin III) for their invaluable help and dedication toward  
488 instrument development, and the crew of the R/V Zephyr for their support and  
489 expertise during field operations. Thanks also to the MBARI Biological  
490 Oceanography Group, especially Reiko Michisaki for help with MBARI mooring data.  
491 Raphael Kudela and lab, John Ryan, Heather Kerkerling, Tom Wadsworth, Tracy Cote  
492 and the NOAA CoastWatch Program and NASA's Goddard Space Flight Center,  
493 OceanColor Web provided and aided in analyses. Thanks to Jim Birch for help with  
494 manuscript preparations.  
495

496 **REFERENCES**

- 497 Behrenfeld M, Boss E (2006). Beam attenuation and chlorophyll concentration as  
498 alternative optical indices of phytoplankton biomass. *Journal of marine research* **64**:  
499 431-451.  
500
- 501 Beman JM, Popp BN, Francis CA (2008). Molecular and biogeochemical evidence for  
502 ammonia oxidation by marine Crenarchaeota in the Gulf of California. *ISME J* **2**: 429-  
503 441.  
504
- 505 Bolin R, Abbott D (1963). Studies on the marine climate and phytoplankton of the  
506 central coastal area of California. *California cooperative oceanic fisheries*  
507 *investigations, progress report (1963)* **9**: 23-45.  
508
- 509 Breaker L, Broenkow W (1994). The circulation of Monterey Bay and related  
510 processes. *Oceanogr Mar Biol Ann Rev* **32**: 1-64.  
511
- 512 Brochier-Armanet C, Boussau B, Gribaldo S, Forterre P (2008). Mesophilic  
513 Crenarchaeota: proposal for a third archaeal phylum, the Thaumarchaeota. *Nat Rev*  
514 *Microbiol* **6**: 245-252.  
515
- 516 Chavez FP (1999). Biological and Chemical Response of the Equatorial Pacific Ocean  
517 to the 1997-98 El Niño. *Science* **286**: 2126-2131.  
518
- 519 Chavez FP, Ryan J, Lluch-Cota SE, Ñiquen C M (2003). From Anchovies to Sardines  
520 and Back: Multidecadal Change in the Pacific Ocean. *Science* **299**: 217-221.  
521
- 522 Doney SC (1999). Major challenges confronting marine biogeochemical modeling.  
523 *Global Biogeochem Cycles* **13**: 705-714.  
524
- 525 Doucette GJ, Mikulski CM, Jones KL, King KL, Greenfield DI, Marin R *et al.*, (2009).  
526 Remote, subsurface detection of the algal toxin domoic acid onboard the  
527 Environmental Sample Processor: Assay development and field trials. *Harmful Algae*  
528 **8**: 880-888.  
529
- 530 Dugdale RC, Goering JJ (1967). Uptake of new and regenerated forms of nitrogen in  
531 primary productivity. *Limnology and Oceanography* **12**: 196-206.  
532
- 533 Francis CA, Roberts KJ, Beman JM, Santoro AE, Oakley BB (2005). Ubiquity and  
534 diversity of ammonia-oxidizing archaea in water columns and sediments of the  
535 ocean. *Proceedings of the National Academy of Sciences of the United States of*  
536 *America* **102**: 14683-14688.  
537
- 538 Goericke R, Welschmeyer NA (1993). The marine prochlorophyte Prochlorococcus  
539 contributes significantly to phytoplankton biomass and primary production in the



540 Sargasso Sea. *Deep Sea Research Part I: Oceanographic Research Papers* **40**: 2283-  
541 2294.  
542  
543 Goffredi SK, Jones WJ, Scholin CA, Marin R, 3rd, Vrijenhoek RC (2006). Molecular  
544 detection of marine invertebrate larvae. *Mar Biotechnol (NY)* **8**: 149-160.  
545  
546 Green RE, Sosik HM, Olson RJ (2003). Contributions of Phytoplankton and Other  
547 Particles to Inherent Optical Properties in New England Continental Shelf Waters.  
548 *Limnology and Oceanography* **48**: 2377-2391.  
549  
550 Green RE, Sosik HM (2004). Analysis of apparent optical properties and ocean color  
551 models using measurements of seawater constituents in New England continental  
552 shelf surface waters. *J Geophys Res* **109**: C03026.  
553  
554 Greenfield DI, Marin R, Doucette GJ, Mikulski C, Jones K, Jensen S *et al.*, (2008). Field  
555 applications of the second-generation Environmental Sample Processor (ESP) for  
556 remote detection of harmful algae: 2006-2007. *Limnology and Oceanography*  
557 *Methods* **6**: 667-679.  
558  
559 Haywood AJ, Scholin CA, Marin III R, Steidinger KA, Heil C, Ray J (2007). Molecular  
560 detection of the brevetoxin-producing dinoflagellate *Karenia brevis* and closely  
561 related species using rRNA-targeted probes and a semiautomated sandwich  
562 hybridization assay. *Journal of Phycology* **43**: 1271-1286.  
563  
564 Johnson KS, Berelson WM, Boss ES, Chase Z, Claustre H, Emerson SR, *et al.*, (2009).  
565 Observing biogeochemical cycles t global scales with profiling floats and gliders.  
566 *Oceanography* **22**: 216-225.  
567  
568 Johnson K, Coletti L, Chavez F (2006). Diel nitrate cycles observed with in situ  
569 sensors predict monthly and annual new production. *Deep Sea Research Part I:*  
570 *Oceanographic Research Papers* **53**: 561-573.  
571  
572 Johnson KS, Coletti LJ (2002). In situ ultraviolet spectrophotometry for high  
573 resolution and long-term monitoring of nitrate, bromide and bisulfide in the ocean.  
574 *Deep-Sea Research Part I-Oceanographic Research Papers* **49**: 1291-1305.  
575  
576 Karl DM, Letelier R, Hebel D, Tupas L, Dore J, Christian J *et al.*, (1995). Ecosystem  
577 changes in the North Pacific subtropical gyre attributed to the 1991-92 El Nino.  
578 *Nature* **373**: 230-234.  
579  
580 Karl DM (1999). Minireviews: A Sea of Change: Biogeochemical Variability in the  
581 North Pacific Subtropical Gyre. *Ecosystems* **2**: 181-214.  
582  
583 Karl DM, Dore JE (2001). Microbial ecology at sea: Sampling, subsampling, and  
584 incubation considerations. *Methods in Microbiology* **30**: 13-27.  
585

586 Karl DM (2007). Microbial oceanography: paradigms, processes and promise.  
587 *Nature Reviews Microbiology* **5**: 759-769.  
588  
589 Karner MB, DeLong EF, Karl DM (2001). Archaeal dominance in the mesopelagic  
590 zone of the Pacific Ocean. *Nature* **409**: 507-510.  
591  
592 Könneke M, Bernhard AE, de la Torre JR, Walker CB, Waterbury JB, Stahl DA (2005).  
593 Isolation of an autotrophic ammonia-oxidizing marine archaeon. *Nature* **437**: 543-  
594 546.  
595  
596 L'Helguen S, Maguer J-F, Caradec J (2008). Inhibition kinetics of nitrate uptake by  
597 ammonium in size-fractionated oceanic phytoplankton communities: implications  
598 for new production and f-ratio estimates. *Journal of Plankton Research* **30**: 1179-  
599 1188.  
600  
601 Liu HB, Nolla HA, Campbell L (1997). Prochlorococcus growth rate and contribution  
602 to primary production in the equatorial and subtropical North Pacific Ocean. *Aquatic*  
603 *Microbial Ecology* **12**: 39-47.  
604  
605 Massana R, Murray A, Preston C, DeLong E (1997). Vertical distribution and  
606 phylogenetic characterization of marine planktonic Archaea in the Santa Barbara  
607 Channel. *Appl Environ Microbiol* **63**: 50-56.  
608  
609 McGowan JA, Cayan DR, Dorman LM (1998). Climate-Ocean Variability and  
610 Ecosystem Response in the Northeast Pacific. *Science* **281**: 210-217.  
611  
612 Mincer TJ, Church MJ, Taylor LT, Preston C, Karl DM, DeLong EF (2007). Quantitative  
613 distribution of presumptive archaeal and bacterial nitrifiers in Monterey Bay and  
614 the North Pacific Subtropical Gyre. *Environmental Microbiology* **9**: 1162-1175.  
615  
616 Mosier AC, Francis CA (2011). Determining the Distribution of Marine and Coastal  
617 Ammonia-Oxidizing Archaea and Bacteria Using a Quantitative Approach. In: Martin  
618 GK (ed). *Methods in Enzymology*. Academic Press. pp 205-221.  
619  
620 Murray AE, Blakis A, Massana R, Strawzewski S, Passow U, Alldredge A *et al.*, (1999).  
621 A time series assessment of planktonic archaeal variability in the Santa Barbara  
622 Channel. *Aquatic Microbial Ecology* **20**: 129-145.  
623  
624 Ottesen EA, Marin III R, Preston CM, Young CR, Ryan JP, Scholin CA *et al.*, (2011).  
625 Metatranscriptomic analysis of autonomously collected and preserved marine  
626 bacterioplankton. *ISME Journal*, doi:10.1038/ismej.2011.70.  
627  
628 Paerl RW, Foster RA, Jenkins BD, Montoya JP, Zehr JP (2008). Phylogenetic diversity  
629 of cyanobacterial narB genes from various marine habitats. *Environmental*  
630 *Microbiology* **10**: 3377-3387.  
631

632 Paerl RW, Johnson KS, Welsh RM, Worden AZ, Chavez FP, Zehr JP (2011).  
633 Differential distributions of *Synechococcus* subgroups across the California Current  
634 System. *Frontiers in Microbiology* **2**.  
635  
636 Paerl RW, Turk KA, Beinart RA, Chavez FP, Zehr JP (in review). Seasonal change in  
637 *Synechococcus* and *Synechococcus narB* subgroup abundances at Monterey Bay  
638 monitoring site M0. *Environmental Microbiology*.  
639  
640 Palenik B, Ren Q, Tai V, Paulsen IT (2009). Coastal *Synechococcus* metagenome  
641 reveals major roles for horizontal gene transfer and plasmids in population  
642 diversity. *Environmental Microbiology* **11**: 349-359.  
643  
644 Paul J, Scholin C, Van Den Engh G, Perry MJ (2007). In situ instrumentation.  
645 *Oceanography* **20**: 70-78.  
646  
647 Pennington JT, Chavez FP (2000). Seasonal fluctuations of temperature, salinity,  
648 nitrate, chlorophyll and primary production at station H3/M1 over 1989-1996 in  
649 Monterey Bay, California. *Deep-Sea Research Part II-Topical Studies in Oceanography*  
650 **47**: 947-973.  
651  
652 Preston C, Harris A, Ryan JP, Roman B, Marin R, Jensen S *et al.*, (2011). Application of  
653 quantitative PCR on a coastal mooring. *PLOS One* **6**: e22522.  
654  
655 Preston CM, Marin R, Jensen SD, Feldman J, Birch JM, Massion EI *et al.*, (2009). Near  
656 real-time, autonomous detection of marine bacterioplankton on a coastal mooring in  
657 Monterey Bay, California, using rRNA-targeted DNA probes. *Environmental*  
658 *Microbiology* **11**: 1168-1180.  
659  
660 Santoro AE, Casciotti KL, Francis CA (2010). Activity, abundance and diversity of  
661 nitrifying archaea and bacteria in the central California Current. *Environmental*  
662 *Microbiology* **12**: 1989-2006.  
663  
664 Scanlan DJ, West NJ (2002). Molecular ecology of the marine cyanobacterial genera  
665 *Prochlorococcus* and *Synechococcus*. *Fems Microbiology Ecology* **40**: 1-12.  
666  
667 Scholin C, Doucette G, Jensen S, Roman B, Pargett D, Marin R *et al.*, (2009). Remote  
668 Detection of Marine Microbes, Small Invertebrates, Harmful Algae, and Biotoxins  
669 Using the Environmental Sample Processor (Esp). *Oceanography* **22**: 158-167.  
670  
671 Scholin C (2010). What are "ecogenomic sensors?" A review and thoughts for the  
672 future. *Ocean Sci* **6**: 51-60.  
673  
674 Shade A, Carey CC, Kara E, Bertilsson S, McMahon KD, Smith MC (2009). Can the  
675 black box be cracked? The augmentation of microbial ecology by high-resolution,  
676 automated sensing technologies. *ISME J* **3**: 881-888.  
677

678 Spang A, Hatzenpichler R, Brochier-Armanet C, Rattei T, Tischler P, Spieck E *et al.*,  
679 (2010). Distinct gene set in two different lineages of ammonia-oxidizing archaea  
680 supports the phylum Thaumarchaeota. *Trends in Microbiology* **18**: 331-340.  
681  
682 Tai V, Palenik B (2009). Temporal variation of Synechococcus clades at a coastal  
683 Pacific Ocean monitoring site. *Isme Journal* **3**: 903-915.  
684  
685 Toledo G, Palenik B (1997). Synechococcus diversity in the California current as  
686 seen by RNA polymerase (rpoC1) gene sequences of isolated strains. *Applied and*  
687 *Environmental Microbiology* **63**: 4298-4303.  
688  
689 Wilhelm SW, Trick CG (1994). Iron-Limited Growth of Cyanobacteria - Multiple  
690 Siderophore Production Is a Common Response. *Limnology and Oceanography* **39**:  
691 1979-1984.  
692  
693 Yool A, Martin AP, Fernandez C, Clark DR (2007). The significance of nitrification for  
694 oceanic new production. *Nature* **447**: 999-1002.  
695  
696 Zehr JP, Waterbury JB, Turner PJ, Montoya JP, Omoregie E, Steward GF *et al.*, (2001).  
697 Unicellular cyanobacteria fix N<sub>2</sub> in the subtropical North Pacific Ocean. *Nature* **412**:  
698 635-638.  
699  
700 Zwirgmaier K, Jardillier L, Ostrowski M, Mazard S, Garczarek L, Vaultot D *et al.*,  
701 (2008). Global phylogeography of marine Synechococcus and Prochlorococcus  
702 reveals a distinct partitioning of lineages among oceanic biomes. *Environmental*  
703 *Microbiology* **10**: 147-161.  
704  
705  
706

707 **FIGURE LEGENDS:**  
708

709 **Figure 1. Environmental data for Monterey Bay** in A) Spring and B) Fall. First  
710 panel includes MODIS 8-day composite satellite images of chlorophyll-*a* for selected  
711 dates during each deployment (most were not available for the spring dates). Star  
712 in right panel is approximate location of Station M0. Color legends range from  
713 (purple to red): 5/18/09: -0.6 to 2.0, 6/3/09: -0.7 to 2.1, 6/12/09: -0.5 to 2.3,  
714 10/01/09: -0.4 to 2.4, 10/08/09: -0.4 to 2.4, and 10/14/09: -0.8 to 1.8. Units are log  
715 mg/m<sup>3</sup>. Panels below contain continuous temperature, nitrate, chlorophyll-*a* and  
716 salinity data gathered from ISUS, CTD sensors coupled with the ESP during each  
717 deployment. The two bloom periods in the spring are designated with a box from  
718 ca. May 24 to June 2 and after June 8. Arrows point to periods of offshore water  
719 influx into the bay.

720

721 **Figure 2. Abundances of bacterial and archaeal gene copy numbers per ml**  
722 **seawater over time** for A) spring and B) fall, 2009, plotted on a log scale. Panels  
723 below show Monterey Bay water column temperature and salinity characteristics  
724 over this period (note the differences in scales between the spring and fall). Dotted  
725 line within each of the bottom panels corresponds with the average deployment  
726 depth for each season.

727

728 **Figure 3. Eukaryotic phytoplankton abundances.** Percent transmission vs.  
729 chlorophyll-*a* for both spring (squares) and fall (diamonds) periods. Top left of  
730 graph indicates high phytoplankton relative to bottom right. The size of the data

731 point within each season corresponds to the time of sampling; the larger the data  
732 point the later it is in the deployment. As described in the text, dark outlined points  
733 are those depicting upwelling relaxation in the spring (squares, mid-deployment)  
734 and of the influx of the offshore water mass in the fall (diamonds, end of  
735 deployment).

736

737 Figure 4. ***Thaumarchaea* population dynamics.** A) Bubble plot of *Thaumarchaea*  
738 abundances (i.e. 16S rRNA gene copy numbers) in the spring (thick outlined) and  
739 fall (no outline) vs. nitrate and chlorophyll-*a* concentrations. Size of bubble  
740 corresponds to the population size; brightness corresponds with time (the darker  
741 the bubble, the earlier in the deployment). Bubbles with dotted outlines indicate  
742 time points corresponding with the period of upwelling relaxation in the spring. B)  
743 *Thaumarchaea* total population abundances (i.e.16S rRNA gene copy numbers in  
744 dark), and *amoA* water column A gene copy numbers (in light) over the fall period,  
745 plotted vs. nitrate and chlorophyll.

746

747 Figure 5. ***Synechococcus* populations and environmental parameters.** Bubble  
748 plot of *Synechococcus* total abundances (i.e. *rbcL* copy numbers) in the spring (dark  
749 outlined) and fall (no outline) vs. nitrate and chlorophyll-*a* concentrations. Size of  
750 bubble corresponds to the population size; brightness corresponds with time (the  
751 darker the bubble, the earlier in the deployment). Bubbles with dotted outlines  
752 correspond to time points corresponding with the period of upwelling relaxation in  
753 the spring. Plus signs correspond with chlorophyll-*a* and nitrate concentrations

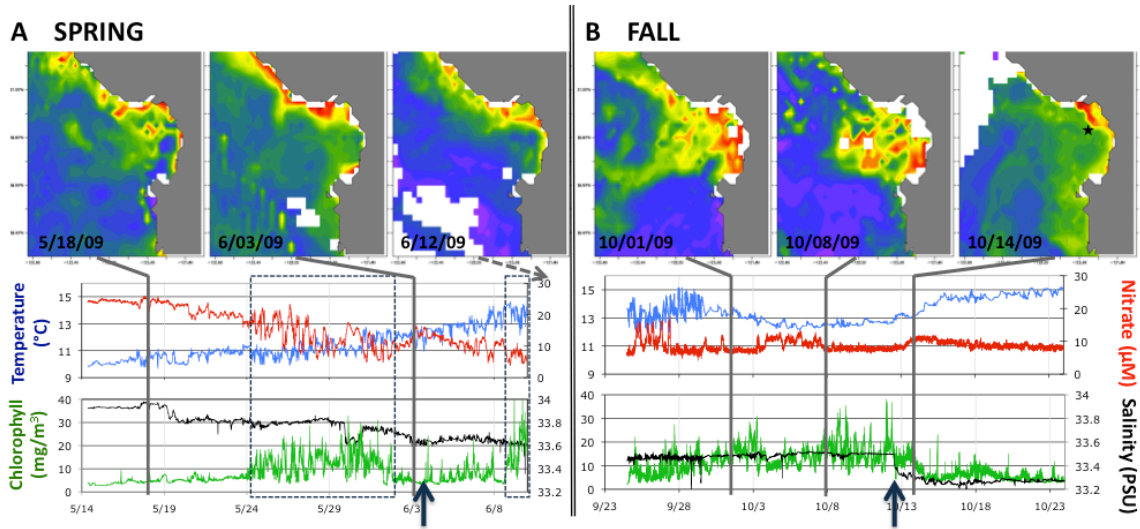
754 sampled by the MBARI Monterey Bay time series at Station M0 over the course of 4  
755 years with ca. 3-week resolution. Dotted box indicates the range of chlorophyll-*a*  
756 and nitrate concentrations where we sampled abundant *Synechococcus*.

757

758 Figure 6. ***Synechococcus* subclade dynamics.** A) *Synechococcus* clade abundances  
759 over time. *narB*, group D\_C2 (black) and group C\_C1 (grey) gene copy numbers  
760 correspond to the *Synechococcus* subclades enumerated in the fall (Sept to Oct,  
761 2009). Arrow points to time of offshore water influx. B) *Synechococcus* total (filled  
762 circles) and subclade (black solid and dotted open circles) abundances with respect  
763 to temperature and salinity in the fall.

764

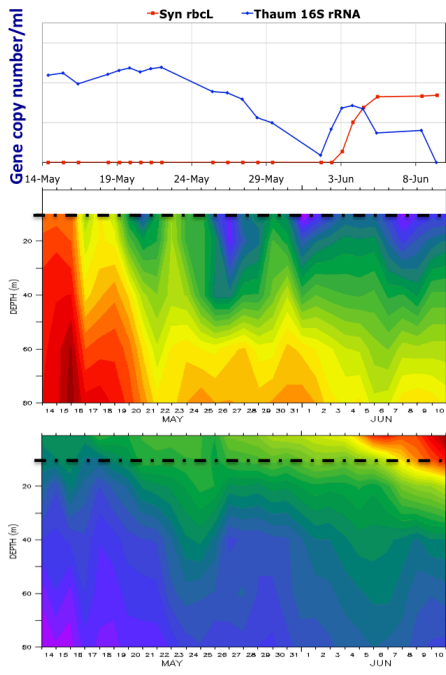
765



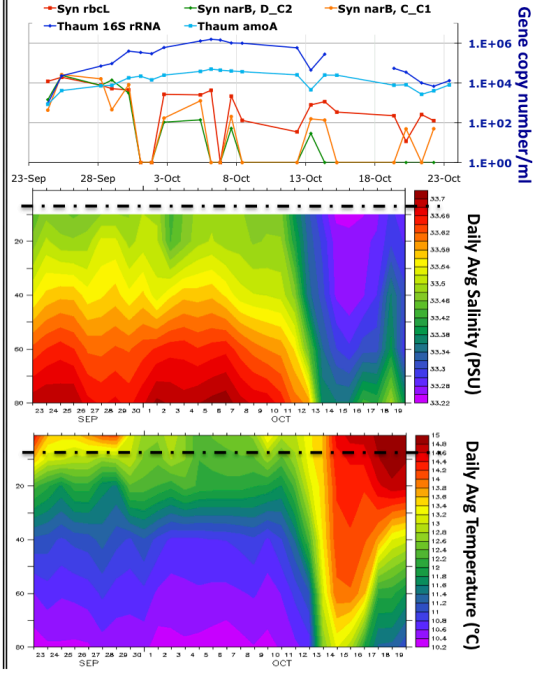
766  
767



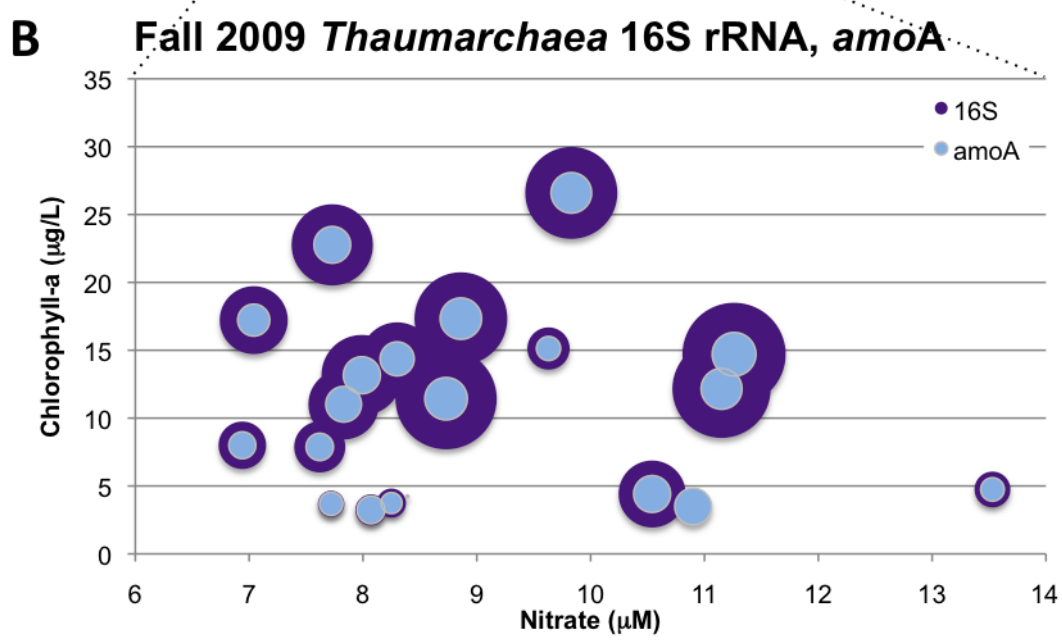
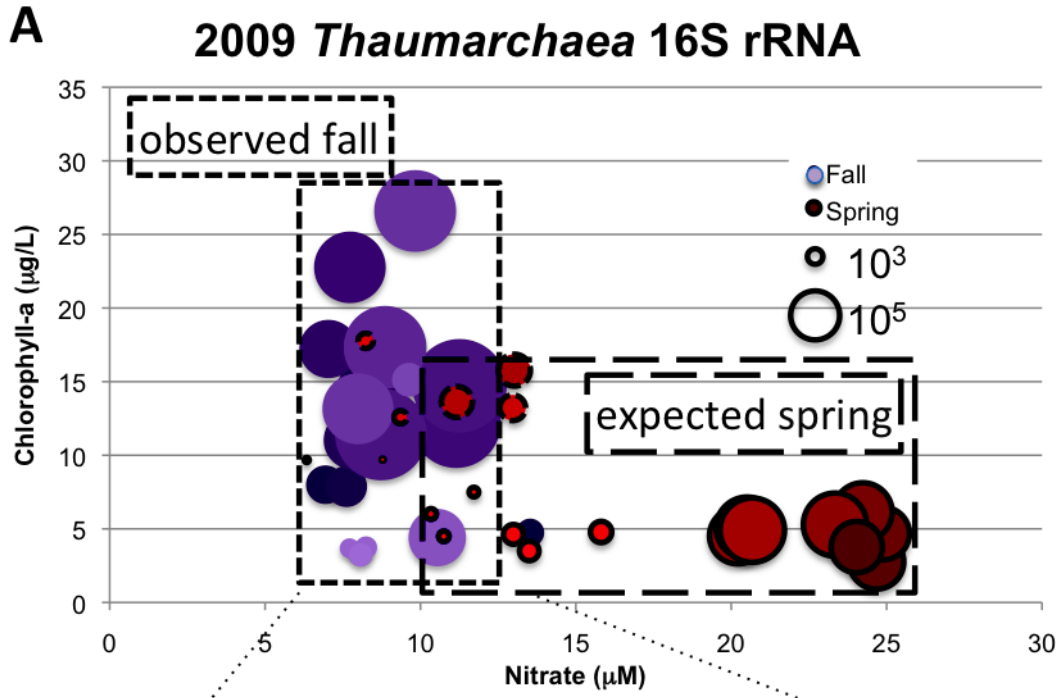
**A SPRING**



**B FALL**



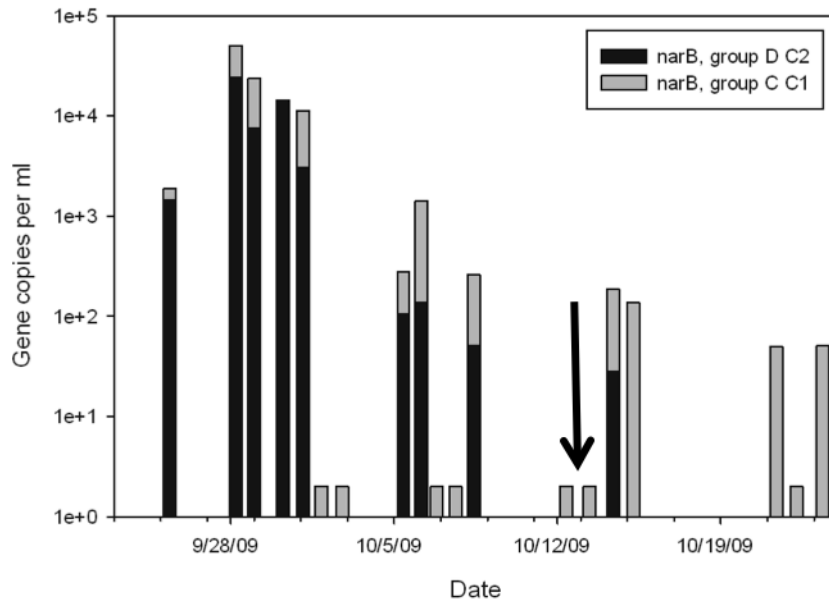
768  
769



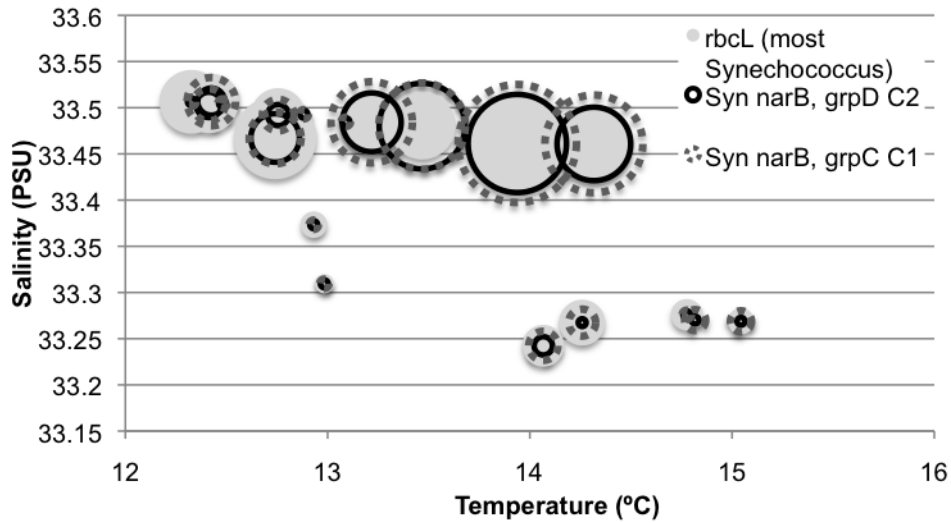
770  
771



**A** Relative abundance of *Synechococcus* clades



**B** Fall 2009 *Synechococcus* *rbcL*, *narB*



774  
775  
776  
777  
778  
779